

Supplementary Materials for

Targeted Tumor-Penetrating siRNA Nanocomplexes for Credentialing the Ovarian Cancer Oncogene *ID4*

Yin Ren, Hiu Wing Cheung, Geoffrey von Maltzhan, Amit Agrawal, Glenn S. Cowley, Barbara A. Weir, Jesse S. Boehm, Pablo Tamayo, Alison M. Karst, Joyce F. Liu, Michelle S. Hirsch, Jill P. Mesirov, Ronny Drapkin, David E. Root, Justin Lo, Valentina Fogal, Erkki Ruoslahti, William C. Hahn,* Sangeeta N. Bhatia*

*To whom correspondence should be addressed. E-mail: william_hahn@dfci.harvard.edu (W.C.H.); sbhatia@mit.edu (S.N.B.)

Published 15 August 2012, *Sci. Transl. Med.* **4**, 147ra112 (2012)
DOI: 10.1126/scitranslmed.3003778

The PDF file includes:

Materials and Methods

Fig. S1. Amplification and overexpression of *ID4* in ovarian cancers.

Fig. S2. *ID4* regulates *HOXA9* gene activity.

Fig. S3. *ID4* regulates expression of *HOXA9* in ovarian cancer cells.

Fig. S4. In vitro characterization of TPNs.

Fig. S5. TPN-mediated suppression of *ID4* in p32-expressing ovarian cancer cells.

Fig. S6. Biodistribution of TPN.

Fig. S7. Therapeutic effects of *ID4* suppression in ovarian tumor-bearing mice.

Fig. S8. Lack of toxicity of si*ID4*.

Table S1. List of amplified genes with at least one shRNA that score with a $P < 0.05$.

Table S2. Sequence and characterization of tandem peptides.

Materials and Methods

Analysis of TCGA primary tumor data

Regions of copy number amplification identified by Genomic Identification of Significant Targets in Cancer (GISTIC) analyses were used from the TCGA study on high-grade serous ovarian cancer (1). All RefSeq genes within these regions of amplification ($n = 1825$) were identified and cross referenced with genes interrogated in the screening library ($n = 778$). All primary high-grade serous ovarian cancer data were downloaded from the TCGA portal (<http://tcga-data.nci.nih.gov/tcga>). The frequency of amplification for *ID4*, *KRAS*, *ERBB3*, and *SKP2* genes was determined by using a threshold of \log_2 copy number ratio > 0.3 within a subset of tumors in TCGA project ($n = 345$). Screenshots of the same tumor data were taken using the Integrative Genome Browser (<http://www.broadinstitute.org/igv>).

Analysis of shRNA screening data

Raw .CEL files from custom Affymetrix barcode arrays were processed with a modified version of dCHIP software. The GenePattern module ‘shRNAscores’ was used to calculate the log fold change scores derived from replicate measurements of the shRNA abundance in each cell line at the conclusion of the screening relative to initial DNA reference pool. This score was adjusted to de-emphasize shRNAs that showed high variability among replicates of the DNA pool. This log fold change score was divided by the s.d. of the DNA pool after it had been mean centered at 1 and floored at 1 to de-emphasize shRNAs that showed high variability among replicates of the DNA pool, which likely arises from technical artifacts including shRNA under-representation in the initial DNA pool or sub-optimal array probe performance. The Gene Pattern module ‘NormalizeCellLines’ was then used to normalize the adjusted log fold change scores among cell lines by scaling and centering these scores with peak median absolute deviation (PMAD) normalization, a variation of ZMAD. PMAD normalization consisted of, first, centering the shRNA scores per cell line at 0 by subtracting the value of each shRNA from the modeled peak value of the distribution of each cell line. The shRNA scores for each cell line were then rescaled so that each line had similar data ranges by dividing the centered data for each shRNA by the median absolute deviation (MAD).

To identify genes that were both amplified in ovarian tumors and essential in amplified cell lines, each gene identified as amplified in primary ovarian tumors was tested across the

entire panel of 102 cell lines screened. For those genes that had 5 or more lines with an amplification of the gene, the median shRNA score for each shRNA in the pool was calculated and used to convert shRNA scores to z -scores. Amplified genes that had mapped shRNAs with a $P < 0.05$ were identified.

Cell culture and generation of stable cell lines

All human cancer cell lines were cultured in previously described media supplemented with 10% fetal bovine serum (FBS, Sigma) (2). Immortalized human ovarian surface epithelial cells (IOSE) (43) were maintained in 1:1 Medium 199: DMEM supplemented with 10% FBS. HeLa, MDA-MB-435, and T22H cells were cultured in Dulbecco's modification of Eagle's medium (Invitrogen) with 10% bovine serum (Invitrogen). An OVCAR-8 cell line stably expressing firefly luciferase was generously provided by J. Liu (Dana-Farber Cancer Institute). Retroviruses were generated by transfection of 293T packaging cells with pBabe/pWzI and pCL-Ampho plasmids (14). Lentiviruses were produced by transfection of 293T packaging cells with a three-plasmid system. To generate stable cell lines, cells were seeded into 10-cm dishes for 24 h before infection with either 5 ml of retroviruses or 0.3 ml of lentiviruses for 3 h in the presence of 4 $\mu\text{g/ml}$ polybrene. After the incubation, medium was replaced with fresh medium for another 24 h before selection in media containing 2 $\mu\text{g/ml}$ of puromycin for 2 days, 10 $\mu\text{g/ml}$ of blasticidin for 4 days, or 800 $\mu\text{g/ml}$ of neomycin for 5 days.

Plasmids

Human *ID1*, *ID2*, *ID3* (from the CCSB human ORFeome collection, Dana-Farber Cancer Institute), and *ID4* (from Origene) were cloned into pLenti6.3-blast (*Bam*HI and *Bsr*GI sites). The *ID4*^{S73P,L94P} (or *ID4_DM*) mutant was generated using the Quikchange Site-Directed Mutagenesis kit (Stratagene). The pLenti6.2-LacZ was used as a control vector. Human *HOXA9* was provided by Anna Schinzel at Dana-Farber Cancer Institute and cloned into pWzI-blast (*Bam*HI and *Eco*RI). The human *HRAS*^{V12} and *KRAS*^{V12} in pBabe-puro vectors have been described (14). The human *MEK*^{D218,D222} (or *MEK*^{DD}) fragment was removed from pBabe-puro-MEK^{DD} plasmid (14) with *Bam*HI and *Sal*I and inserted into pBabe-neomycin. Lentiviral pLKO.1-puro-shRNA constructs were obtained from The RNAi Consortium. The shRNA constructs used are as follows: control shRNA targeting *GFP* (TRCN0000072181), *ID4*-specific shRNAs (sh*ID4*#1: TRCN0000017323, sh*ID4*#2: TRCN0000071444 and sh*ID4*#3:

TRCN0000017325), and *HOXA9*-specific shRNAs (sh*HOXA9*#1: TRCN0000012509, sh*HOXA9*#2: TRCN0000012510, sh*HOXA9*#3: TRCC0019251728, sh*HOXA9*#4: TRCC0019251729).

Peptides and siRNAs

The tandem peptide library was synthesized via standard Fmoc solid-phase peptide synthesis and purified by high-performance liquid chromatography at the MIT Biopolymers Core, Tufts University Core Facility or CPC Scientific, Inc. The tandem peptides were then cyclized by bubbling air into 3 μ M aqueous peptide solutions for 24 h, followed by lyophilization and storage at -80°C for later use. All siRNAs were obtained from Dharmacon, Inc. The sequences of siRNAs (5'-3') are as follows: si*GFP* (GGCUACGUCCAGGAGCGCA), si*LUC* (CUUACGCUGAGUACUUCGA), si *β gal-728* (CUACACAAAUCAGCGAUUU), si*ID4_568* (GAUAUGAACGACUGCUAUA), si*ID4_621* (CAACAAGAAAGUCAGCAAA), si*ID4_564* (GUGCGAUAUGAACGACUGCUA), and si*ID4_1195* (CCGACUUUAGAAGCCUACUUU).

Fluorescent labelling of siRNA

siRNAs bearing 3'-amine on the sense strand was reacted in PBS with twenty-fold molar excess of Vivotag S-750 amine-reactive dye (Visen Medical, Inc.) for 1 h at 37°C. The reaction mixture was then precipitated overnight at -20°C in 0.5 M NaCl and 40% ethanol. Precipitated siRNA was pelleted through centrifugation at 8000 \times g for 20 minutes at 4°C, washed once with 70% ethanol, and centrifuged again before being air-dried. This labelling process was repeated to yield approximately 3.5 fluorophores per siRNA duplex.

Gene expression profiling

OVCAR-8 cells (2×10^5) were infected with lentiviruses expressing a control shRNA targeting *GFP* (sh*GFP*) or two *ID4*-specific shRNAs (sh*ID4*#1 and sh*ID4*#2) for 24 h. Cells were then cultured in fresh medium containing puromycin for 48 h to select transduced cells (the pLKO.1 vector also encodes the puromycin resistance gene). Total RNA was extracted by Trizol reagent (Invitrogen) followed by RNeasy column purification (Qiagen).

For overexpression experiments, immortalized ovarian serous epithelial cells expressing activated MEK (IOSE-M) cells were subjected to a 3 h infection with lentiviruses expressing control vector or *ID4*. Cells were then cultured in medium containing blasticidin (blasticidin

resistance gene encoded in the pLenti6.3-blast vector) for 4 days to generate polyclonal populations of stable lines and passaged twice before set-up for total RNA extraction. Cells (4×10^5) expressing the indicated constructs were plated onto 10-cm dishes for 48 h and total RNA was extracted as described above. Gene expression profiling was then performed on Affymetrix HG-U133A_2 GeneChips by the Microarray Core at the Dana-Farber Cancer Institute. Probes were aligned to a transcript database consisting of RefSeq (36.1) and complete coding sequences from GenBank (v.161). Gene-centric expression values were generated for every gene with at least 5 probes. Data for each experiment was normalized and summarized using robust multichip average (RMA), then logged and row-normalized.

Gene Set Enrichment Analysis (GSEA)

Processed expression data from either the sh*ID4* or *ID4* overexpression experiments was analyzed using GSEA v2.06 (<http://www.broadinstitute.org/gsea/>) (44). For the shRNA experiments, we compared expression profiles derived from OVCAR-8 cells infected with a control sh*GFP* and OVCAR-8 cells infected with sh*ID4*. For overexpression experiments, IOSE-M cells expressing a control vector were compared to cells overexpressing *ID4*. GSEA was run using the default settings, except for the following; permutations were based on the gene sets, not on phenotype and data was not collapsed to gene symbols (this was done prior to GSEA).

We additionally identified gene sets enriched in particular populations of ovarian tumor samples. GSEA comparing 109 samples with amplified *ID4* (\log_2 copy number ratio >0.3) vs. 81 non-amplified *ID4* samples (\log_2 copy number ratio <0) was performed using expression data from primary ovarian samples with matched copy number from TCGA.

Fluorescence in situ hybridization (FISH)

BAC RP11-72I11 clone containing *ID4* (Invitrogen) was labeled with Digoxigenin (Roche) using BioPrime labeling mix (Invitrogen). A reference probe specific for the centromeric region of Chromosome 6 (CEP6 SpectrumOrange Probe, #06J36-016) was purchased from Abbott Molecular. Labeled DNA was precipitated at -80°C for 2 h with 1 μl of glycogen (20 $\mu\text{g}/\mu\text{l}$), pelleted by centrifugation at $18,000 \times g$ for 15 min at 4°C , air-dried for 10 min, and resuspended in 50 μl of hybridization buffer (50% deionized formamide, 10% dextran sulfate, $2 \times \text{SSC}$).

Slides containing metaphase chromosomes were pretreated with 1:25 Digest-All III (Invitrogen) at 37°C for 6 min before fixation in 10% buffered formalin for 1 min at room

temperature. Slides were dehydrated for 2 min each in 70%, 85%, 95% and 100% ethanol at room temperature. Probes were prepared by mixing 2 μ l of each labeled probe, 1 μ l Cot-1 DNA (1 mg/ml; Invitrogen), and 11 μ l of hybridization buffer. Probes were applied to air-dried slides; coverslips were applied and sealed with rubber cement. These preparations were denatured at 72°C for 5 min. Hybridization was performed for 18 h at 37°C in a dark humid chamber. Coverslips were gently removed and slides were washed in 0.5 \times SSC at 72°C for 5 min, rinsed at room temperature in 1 \times PBS containing 0.025% Tween-20. Slides were blocked with CAS-Block containing 10% normal goat serum (Invitrogen) and then incubated with FITC-anti-Digoxigenin (Roche). Slides were washed in 1 \times PBS containing 0.025% Tween-20 and counterstained with DAPI (Invitrogen). Images were captured by using Zeiss Axio Observer Z1 microscope (Zeiss) and AxioVision digital imaging software (Zeiss).

Gel-shift and stability assays

For the gel-shift assay, siRNA was mixed with peptide at specified molar ratios in phosphate buffered saline for 10–15 min at room temperature. The mixture was analyzed by non-denaturing gel electrophoresis using a 15% acrylamide gel for siRNA, stained with SYBR-Gold, and visualized under UV light. For the siRNA stability assay, siRNA (100 pmol) was mixed with TP-LyP-1 (2 nmol) in PBS for 10–15 min at room temperature. Naked siRNA or TPN was then added to 100% murine serum (10:1 v/v) and incubated at 37°C for the indicated times, after which the RNA was extracted and precipitated, separated on a 15% TBE gel, stained with SYBR-Gold, and visualized under UV light.

Peptide uptake and gene silencing

For the initial screen, HeLa cells expressing GFP were cultured in 96-well plates to ~40-60% confluence. siRNA (0-100 nM) was incubated with 20-fold molar excess of tetramethylrhodamine-labeled tandem peptides in PBS for 10-15 min at room temperature, incubated over cells for 4 h at 37 °C, after which the medium was replaced. Transfection with Lipofectamine RNAiMAX was used as a positive control. The cells were cultured for an additional 24-48 h before being examined by flow cytometry on a BD LSRII instrument. % Knockdown based on the geometric mean of GFP fluorescence of the entire population was normalized to GFP signal of mock treated cells. For competition experiments with free LyP-1

peptide, cells were pre-incubated with unlabeled LyP-1 or ARAL control peptide at specified concentrations from 5 to 20 μM for 1 h at 37 °C before nanocomplex treatment.

For *ID4* gene silencing, siRNAs targeting different exons of the *ID4* mRNA (100 pmol) were mixed with TP-LyP-1 peptide at a molar ratio of 1:20 (siRNA:peptide) in PBS. The mixture was added to OVCAR-8 or OVCAR-4 cell cultures (plated at 0.2×10^6 cells in 6-well plates 48 h prior) for 4-6 h at 37°C and was then replaced with fresh serum-containing media. Cell lysates were collected 48 h later for immunoblotting.

Cell proliferation assay

Eight hundred each of OVCAR-8 and IGROV1 cells, 1000 each of OVCAR-4, SKOV-3, U251-MG, LN-229, HCC827, and DLD-1 cells, 1500 each of CaOV-3, NIH:OVCAR-3, OV-90, MCF7, and T47D cells, and 2000 each of RMG-I, TOV-21G, TOV-112D cells were seeded into each well of 96-well plates 24 h prior to infection. Six replicate infections were performed for control shRNAs and each gene-specific shRNA in the presence of 4 $\mu\text{g/ml}$ polybrene for 24 h followed by selection with 2 $\mu\text{g/ml}$ of puromycin. The ATP content was measured at 6 days post-infection by using CellTiter-Glo luminescent cell viability assay (Promega).

To measure the cytotoxicities of nanocomplexes in vitro, HeLa cells grown in 96-well plates at 40-60% confluency were incubated in triplicate with specified concentrations of nanocomplex formulations in serum-free media for 24 h. Viability was measured using CellTiter-Glo luminescent viability assay (Promega). To measure the cytotoxicity of *ID4* suppression, OVCAR-8 and OVCAR-4 cells grown in 6-well plates at 40-60% confluence were transfected twice on two consecutive days with nanocomplexes containing siRNA against *ID4* (100 pmol) or containing siRNA against GFP. Twenty-four hours after the second transfection, cells were trypsinized and plated in 96-well plates in quadruplicate. The plates were analyzed 24 h later using Celltiter-Glo assays (Promega) according to manufacturer's instructions.

Anchorage-independent growth assay

Growth in soft agar was determined by plating 1×10^4 cells in triplicate in 5 ml of medium containing 0.35% Noble agar (BD Biosciences) which was placed on top of 4 ml of solidified 0.7% agar. Colonies greater than 100 μm in diameter were counted 4 weeks after plating.

Flow cytometry

Fluorescence-activated cell sorting (FACS) analysis of cell-surface p32 was done on live HeLa, MDA-MB-435, OVCAR-4, OVCAR-8, CaOV-3, and T22H cells. Approximately 2.5×10^5 cells were stained with a polyclonal anti-full-length/*N*-terminal p32 or rabbit IgG isotype control (1 μ g per 1×10^6 cells) and Alexa-647 goat anti-rabbit secondary antibody, each for 45 min at 4°C, analyzed by gating for propidium iodide-negative (live) cells.

For analysis of apoptosis, cells were resuspended in 1x Annexin-V binding Buffer (BD Bioscience). Cells were incubated with Annexin-V-FITC and propidium iodide for 15 minutes in the dark according to the manufacturer's recommendation. Binding buffer was added and Annexin-V-positive cells were analyzed by flow cytometry on a BD LSR II instrument.

For analysis of cells entering S-phase, cells were washed with PBS and percentage of cells in S-phase was determined using the Click-iT EdU cell proliferation assay (Invitrogen) according to manufacturer's instructions and analyzed by flow cytometry (BD LSR II).

Immunoblotting

Cell lysates were prepared by scraping cells in lysis buffer [50 mM Tris HCl (pH 8), 150 mM NaCl, 1% Nonidet P40, 0.5% sodium deoxycholate and 0.1% SDS] containing complete protease inhibitors (Roche) and phosphatase inhibitors (10 mM Sodium Fluoride and 5 mM Sodium Orthovanadate). Protein concentration was measured by using BCA Protein Assay kit (Pierce). An equal amount of protein (30 μ g) was separated by NuPAGE Novex Bis-Tris 4-12% gradient gels (Invitrogen) and then transferred onto a polyvinylidene difluoride membrane (Amersham). The membrane was then incubated with primary antibody for 1 h at room temperature. Antibodies against ID1 (sc-488), ID2 (sc-489), ID3 (sc-490), ID4 (sc-13047), K-RAS (sc-30), and H-RAS (sc-29) were purchased from Santa Cruz Biotechnology. Antibodies specific for Caspase-3 (#9665), MEK (#9122), PARP (#9532), and phospho-ERK1/2 (#9101) were from Cell Signaling Technology. Antibody specific for HOXA9 (#07-178) was from Millipore. Antibody specific for α -tubulin (#13-8000) was from Invitrogen.

After incubation with the appropriate HRP-linked secondary antibodies (Bio-Rad), signals were visualized by enhanced chemiluminescence plus Western blotting detection reagents (Amersham). Expression of β -actin was also assessed as an internal loading control by

using a specific antibody (sc-8432-HRP, Santa Cruz). Intensities of bands were quantified by LabWorks image analysis software (UVP) or ImageJ (NIH).

Real-time quantitative RT-PCR

Total RNA was extracted with Trizol reagent (Invitrogen). Total RNA (4 µg) for each sample was used to synthesize the first-strand cDNA by using Oligo(dT)₂₀/random hexamer primer cocktails and SuperScript III reverse transcriptase (Invitrogen). Quantitative RT-PCR reactions were performed using SYBR green PCR Master Mix (Applied Biosystems). The primer sequences used were as follows: *ID4* (forward: 5'-CCGAGCCAGGAGCACTAGAG-3', reverse: 5'-CTTGGGAATGACGAATGAAAACG-3'); *HOXA3* (forward: 5'-TGCTTTGTGTTTTGTCGAGACTC-3', reverse: 5'-CAACCCTACCCCTGCCAAC-3'); *HOXA7* (forward: 5'-TATGTGAACGCGCTTTTTAGCA-3', reverse: 5'-TTGTATAAGCCCGGAACGGTC-3'); *HOXA9* (forward: 5'-GAGTGGAGCGCGCATGAAG-3', reverse: 5'-GGTGACTGTCCCACGCTTGAC-3'); and *GAPDH* (forward: 5'-CCTGTTCGACAGTCAGCCG-3', reverse: 5'-CGACCAAATCCGTTGACTCC-3'). Triplicate reactions for the gene of interest and the endogenous control (*GAPDH*) were performed separately on the same cDNA samples by using the ABI 7900HT real-time PCR instrument (Applied Biosystems). The mean cycle threshold (Ct) was used for the $\Delta\Delta C_t$ analysis method.

Tumorigenicity assay

Female Balb/c and NCR/nude mice (Charles River Laboratories) were obtained at 4-6 weeks of age. All animal experiments were approved by the MIT Committee on Animal Care under approved protocols. Tumor xenograft experiments were performed as described (68). IOSE cell lines expressing indicated constructs were trypsinized and collected in media supplemented with 10% FBS. Cells (8×10^6) were resuspended in 400 µl of 1× PBS and mixed with 400 µl of BD Matrigel-Basement Membrane Matrix, LDEV-free (BD Biosciences) prior to injection. Two hundred µl of the cell mixture (containing 2×10^6 cells) was injected subcutaneously into 8-week-old female BALB/c nude mice. Tumor injection sites were monitored for 5 months for tumor formation. Mice were euthanized when tumors reached 1.5 cm in diameter.

For HOXA9 experiments, *ID4*-overexpressing IOSE-M cells were infected with lentiviruses expressing control shRNAs or sh*HOXA9*#1 or sh*HOXA9*#2. Cells were then cultured in fresh medium for 24 h before selection in 2 µg/ml of puromycin for 2 days. Infected cells were then passaged once before injection into immunodeficient mice as described above.

Systemic administration and in vivo characterization of TPN

Female NCR/nude mice were injected subcutaneously on the bilateral flanks with 2×10^6 MDA-MB-435 melanoma or 2×10^6 OVCAR-8 ovarian cancer cells mixed with Matrigel and allowed tumors to form over two weeks. For circulation and tumor targeting experiments, 5 nmol of near-infrared fluorophore (VivoTag-750)-labeled siRNA was complexed to tandem peptides at a molar ratio of 1:20 in 5% glucose and injected either intravenously or intraperitoneally. Mice were imaged at specified times using the IVIS 200 imaging system (Caliper Life Sciences). Blood was drawn retroorbitally and siRNA fluorescence was measured using the Odyssey imaging system (Li-COR Biosciences). Organs were harvested and imaged 6 h after injection. Tumor explants were examined at high resolution (84 µm) using the Odyssey imager with an excitation wavelength of 785 nm. To study time-dependent homing and tumor, TPNs carrying FITC labeled-siRNA were administered intravenously to OVCAR-8 tumor bearing mice (5 nmol siRNA per injection). Tumors were collected 6 h later for analyses by immunofluorescence or quantification of total injected dose.

To determine the % injected dose accumulated in the tissue, organs and tumors harvested from mice were pulverized under liquid nitrogen and homogenized in 10 mM Tris buffer with 1% SDS. The homogenate was heated at 95°C for 10 minutes and centrifuged at $14,000 \times g$. Fluorescence of the lysate was measured using the Odyssey imager. To generate a standard curve for each organ, organs and tumors from uninjected animals were processed and known amounts of fluorescent siRNAs were spiked into the lysates. The lysates were imaged under the same settings, and the integrated fluorescence intensities versus siRNA concentrations were fitted with a 3-parameter exponential equation: $f = y_0 + a(1 - e^{-bx})$ (SigmaPlot).

Animal models of metastatic ovarian cancer

For the OVCAR-4 tumor model, 3×10^6 OVCAR-4 cells mixed with Matrigel were implanted in the subcutaneous space on the bilateral flanks of 4-6-week-old NCr/nude mice (Charles River

Laboratories). Once tumors were established, animals were divided into treatment cohorts of five mice each, receiving injections of 1 mg siRNA/kg every 3 days for 25 days.

For the OVCAR-8 tumor model, OVCAR-8 cells expressing firefly luciferase were injected intraperitoneally into 4-6-week-old NCr/nude mice (Charles River Laboratories) at 0.5×10^6 cells per mouse. Three weeks later, tumor establishment was confirmed by bioluminescence imaging. The animals were then randomly divided into cohorts of five mice each. The treatment cohort received TPN containing *siID4* (5 mg siRNA/kg/injection). The control cohorts received saline, TPN/*siGFP*, or UCN/*siID4*. siRNA was mixed with peptide at a molar ratio of 1:20 in 200 μ l of water with 5% glucose, and injected intraperitoneally. Treatments were initially twice weekly for 14 days. Upon observing suppression in tumor growth, treatment frequency was reduced to once weekly for 3 more weeks to limit possible side effects and toxicity. On day 60, tumors and organs were harvested for immunohistochemical analyses. Whole-animal BLI was performed every 3 days. Mice were anesthetized using isoflurane, injected with 150 mg/kg D-luciferin (Promega), and imaged 10-15 min after injection once the signal peaked.

Immunostaining and analysis

Tumors were harvested and fixed in 4% paraformaldehyde at 4°C overnight, soaked in 30% (w/v) sucrose for 24 h, then snap frozen. Rat anti-mouse CD31 (1:50, BD PharMingen) and a polyclonal anti-p32 antibody were used for immunohistochemical staining. Rat or rabbit IgGs were used as isotype controls. Sections were washed and detected with Alexa Fluor 488 goat anti-rat or anti-rabbit IgG (1:1000; Invitrogen). The slides were counterstained with DAPI and mounted on glass slides for microscopic analysis. At least three images from representative microscopic fields were analyzed for each tumor sample using the ImageJ software.

Immunogenicity studies in mice

Balb/c immunocompetent mice were injected intraperitoneally with TPN carrying *siID4*, *siGFP*, *siLUC*, or *si β gal-728* at 5 mg siRNA/kg. *si β gal-728* was encapsulated in Lipofectamine. RNAiMAX was used as a positive control. Serum samples obtained 6 h after injections were processed for measurements of IFN- α , TNF- α , and IL-6 by ELISA (PBL Biomedical Laboratories and BD Biosciences) in accordance with the manufacturer's instructions.

SUPPLEMENTARY FIGURES

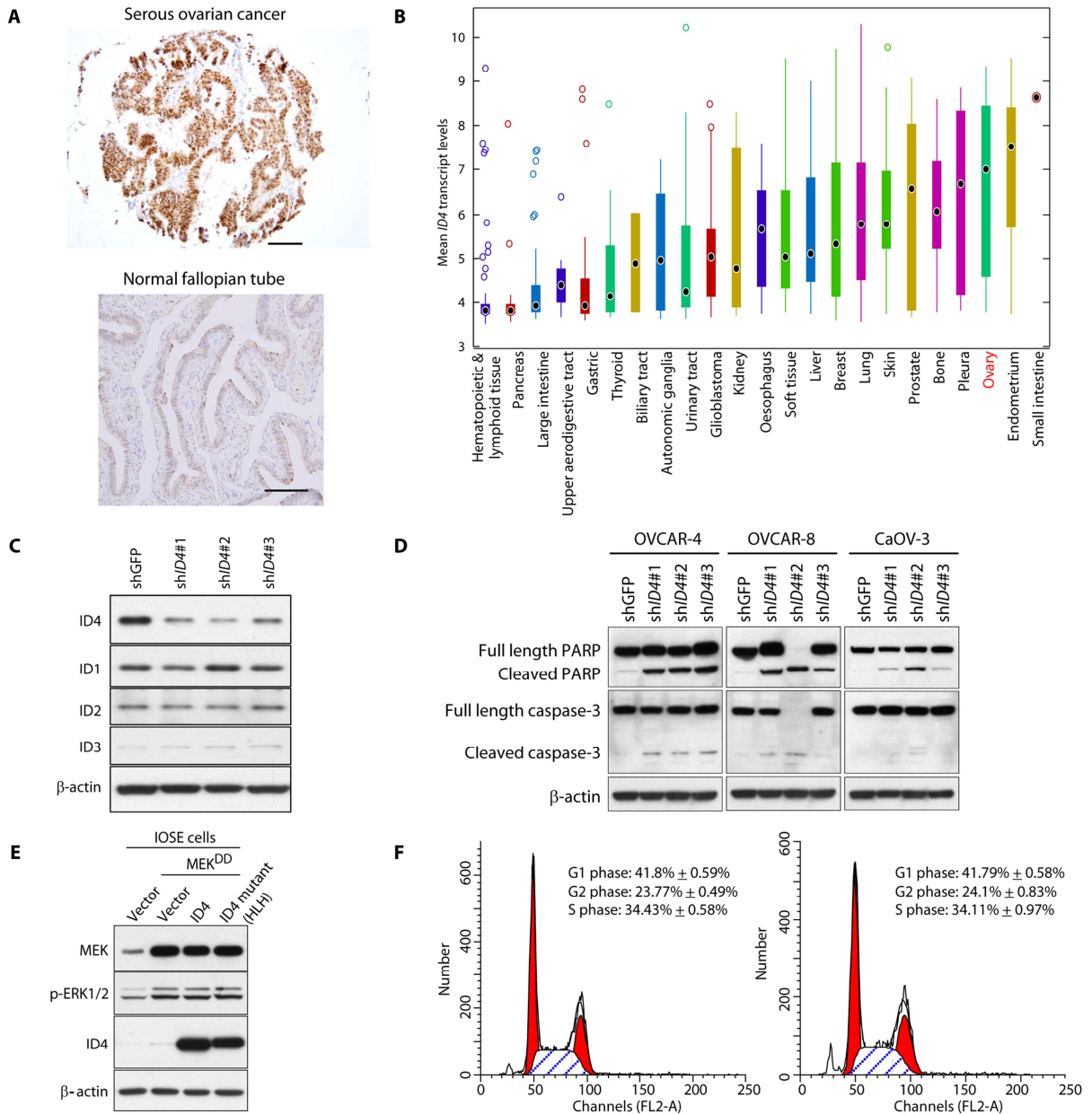


Figure S1. Amplification and overexpression of *ID4* in ovarian cancers. (A) Representative micrographs of a primary serous ovarian cancer (top) and normal fallopian tube (bottom) stained with an anti-*ID4* antibody. Scale bar, 100 μ m. (B) Box plot showing *ID4* expression in human cancer cell lines derived from different lineages (cell lines found at <http://www.broadinstitute.org/ccle>). The black dot in each box plot is the median expression value for each lineage ($n = 765$ data points). Boxes represent the 25th to 75th percentile of the data, and whiskers span the most extreme values of the group. (C) Immunoblot of *ID1*, *ID2*, *ID3*, and *ID4* in human OVCAR-4 cells expressing a control shRNA targeting GFP or 3 different

ID4-specific shRNAs. **(D)** Immunoblot of PARP and caspase-3 after suppressing *ID4* in 6p22-amplified ovarian cancer cell lines. **(E)** Immunoblot of MEK, phospho-ERK1/2, and ID4 in immortalized ovarian surface epithelial cells expressing indicated constructs (IOSE-M cells). **(F)** Cell cycle distribution of IOSE-M cells overexpressing *ID4* (right) or a control vector (left). Data are averages \pm s.d.

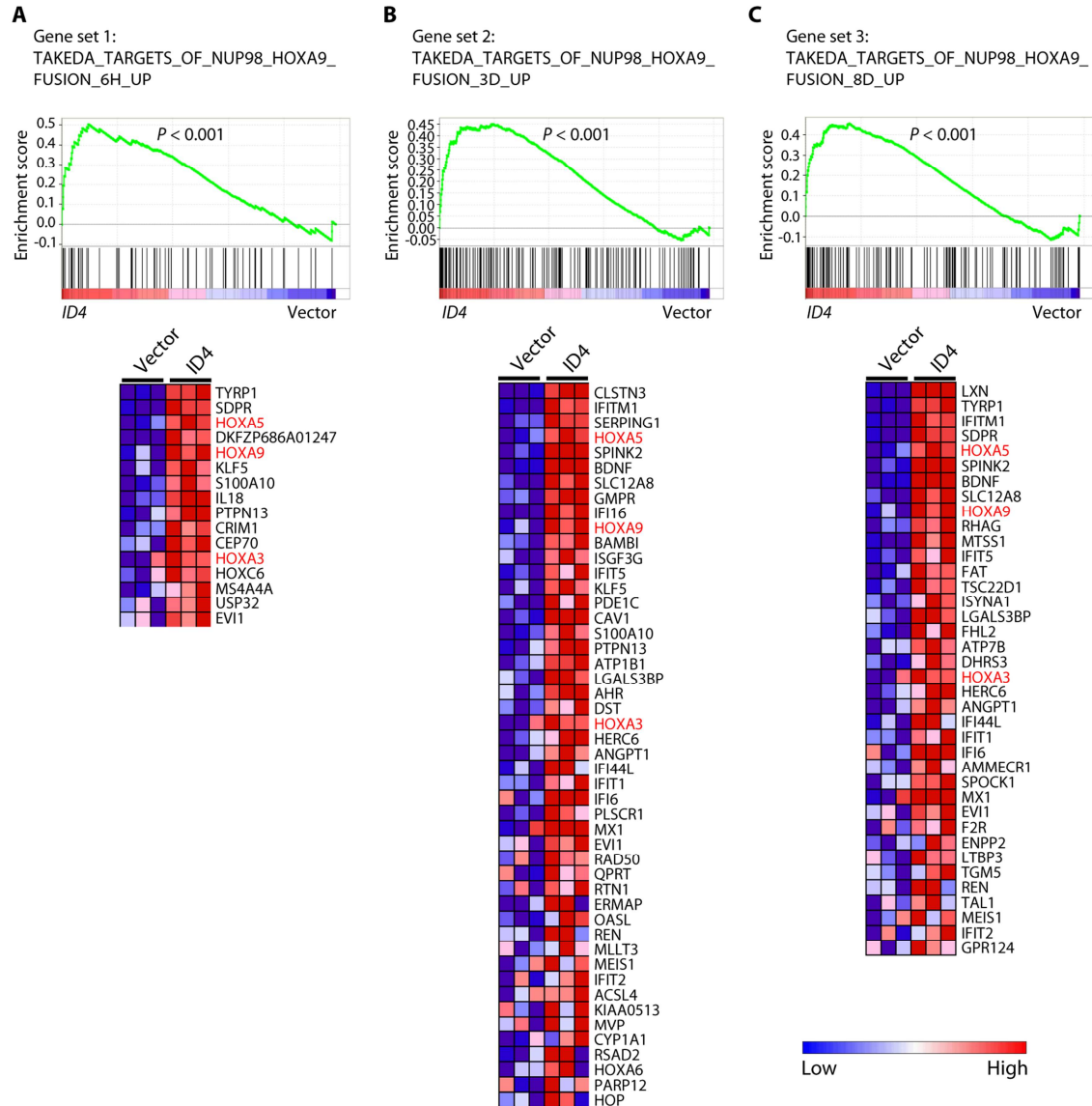


Figure S2. *ID4* regulates *HOXA9* gene activity. Gene expression profiling and GSEA were performed on IOSE-M cells expressing *ID4* or a control vector. (A to C) Enrichment plots (top) show the running enrichment score in green for the ranked list of genes (*x*-axis) on the basis of the differential expression between cells expressing *ID4* or a control vector. Black bars at the bottom of the figure indicate the location of genes in a gene set upregulated by expression of *NUP98-HOXA9* fusion protein generated at 6 hours (A), 3 days (B), and 8 days (C) after induction within the ranked list. Heat maps show the expression levels induced by *ID4* overexpression (triplicate measurements) of a subset of genes within each of the gene set (bottom). Members of the homeobox family of transcription factors are marked in red text. Permutation test was used to calculate the *P* values.

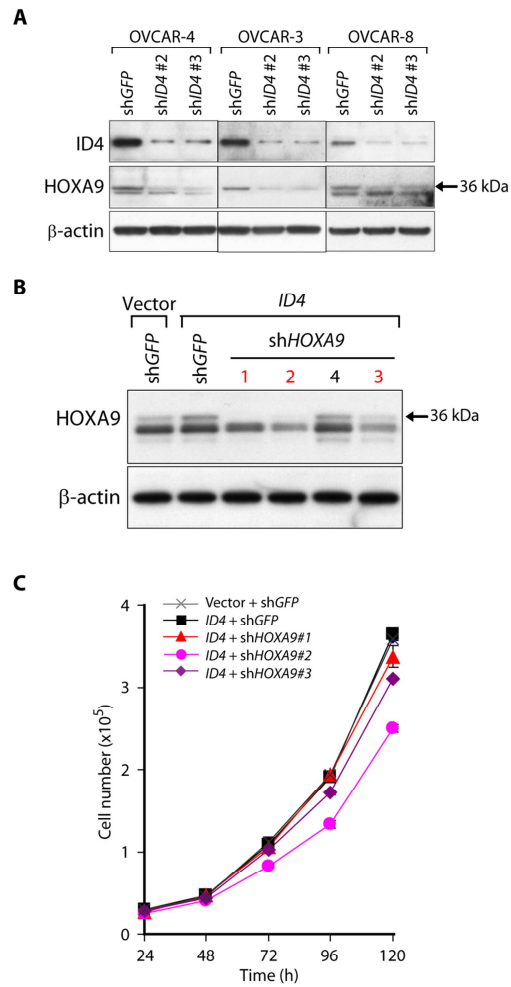


Figure S3. *ID4* regulates expression of *HOXA9* in ovarian cancer cells. (A) Suppression of *ID4* reduces expression of *HOXA9* proteins. Immunoblot of *ID4* or *HOXA9* in OVCAR-4, NIH:OVCAR-3, and OVCAR-8 cells expressing shGFP or sh*ID4*. Arrow indicates the specific *HOXA9* band (36 kDa). β -actin was included as a loading control. (B) Suppression of *HOXA9* protein levels in IOSE-M cells expressing the indicated constructs. Immunoblot of *HOXA9* in IOSE-M cells expressing a control shGFP or *HOXA9*-specific shRNAs. (C) Effect of suppressing *HOXA9* on proliferation of IOSE-M cells. Cells expressing indicated constructs were plated in triplicate and counted daily.

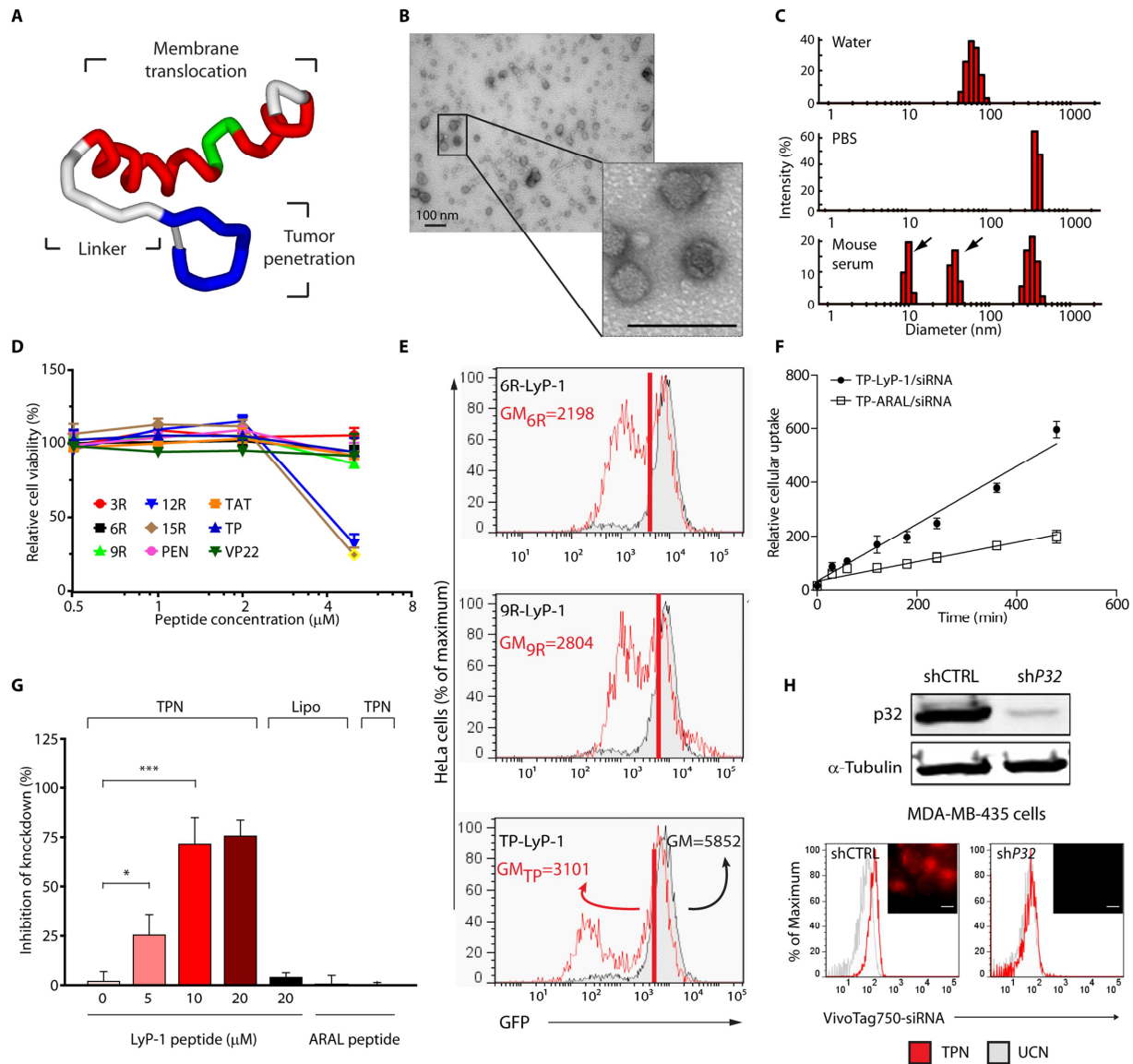


Figure S4. In vitro characterization of TPNs. (A) Schematic diagram of the anticipated structure of a tandem peptide. The cyclic tumor-penetrating domain LyP-1 at the C terminus is separated from the membrane translocation domain (cell-penetrating peptide, CPP) at the N terminus by a (Gly)₄ linker. siRNA associates with the membrane translocation domain. (B) Dynamic light scattering measurements of TPN size in water, PBS, and mouse serum (50 vol% in PBS). Arrows indicate peaks due to serum proteins. (C) Transmission electron micrograph of TPNs in water. A higher magnification view is shown on the right. Scale bars, 100 nm. (D) Cytotoxicity assessments of tandem peptides 48 h after transfection in HeLa cells. Data are averages \pm s.d. ($n = 3$ independent experiments). Total viability was normalized to untreated HeLa cells. (E) Flow cytometry histograms of HeLa cells expressing GFP 24 hours after transfection with tandem peptides (6R-LyP-1, 9R-LyP-1, or TP-LyP-1) carrying GFP-siRNA (100 nM). Mock-treated cells are shown in gray. Geometric mean (GM) of the cell population is indicated with a red vertical line. The GM of the mock-treated cells is shown in black text for TP-LyP-1. (F) Flow cytometry analysis of HeLa cellular uptake of TP-LyP-1/siRNA and TP-

ARAL/siRNA over time. Data are averages \pm s.d. ($n = 3$ independent experiments). **(G)** Competition assay for TPN-mediated GFP gene silencing in HeLa cells treated with siRNA delivered using TP-LyP-1 (TPN) or lipofectamine (Lipo) in the presence of free LyP-1 peptide or a scrambled control peptide (ARAL). Data are averages \pm s.d ($n = 6$ independent measurements). * $p < 0.05$; *** $p < 0.001$, one-way ANOVA. **(H)** p32-dependence of TPN cellular uptake. Immunoblot of MDA-MB-435 cells stably expressing p32-specific shRNA (shP32) or a control shRNA (shCTRL) (top). α -Tubulin was used as a loading control. Cellular uptake of TPN or untargeted control nanocomplexes (UCN) in shP32- or shCTRL-expressing MDA-MB-435 cells (bottom). Insets: Immunofluorescence of cellular uptake of TP-LyP-1 or TP-ARAL carrying siRNA labeled with a near-infrared fluorophore (VivoTag-750, pseudocolored red). Scale bars, 50 μ m.

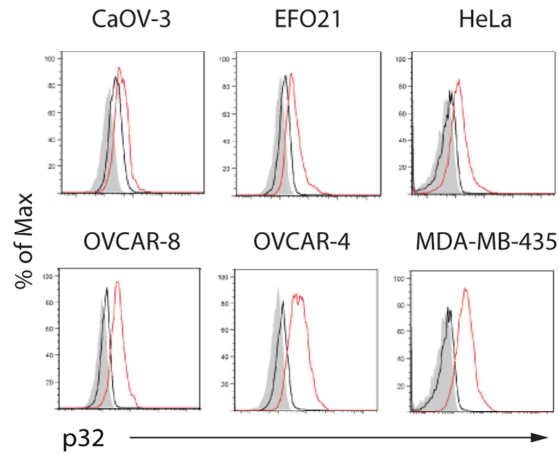


Figure S5. TPN-mediated suppression of *ID4* in p32-expressing ovarian cancer cells. Surface expression of p32 in cancer cell lines. Seven cancer cell lines derived from human ovarian cancer (CaOV-3, EFO21, OVCAR-8, and OVCAR-4), human cervical cancer (HeLa), human melanoma (MDA-MB-435), and mouse ovarian cancer (T22H) were surveyed for surface expression of p32 by flow cytometry (red). An IgG isotype control is in black. Unstained cells are shaded in gray.

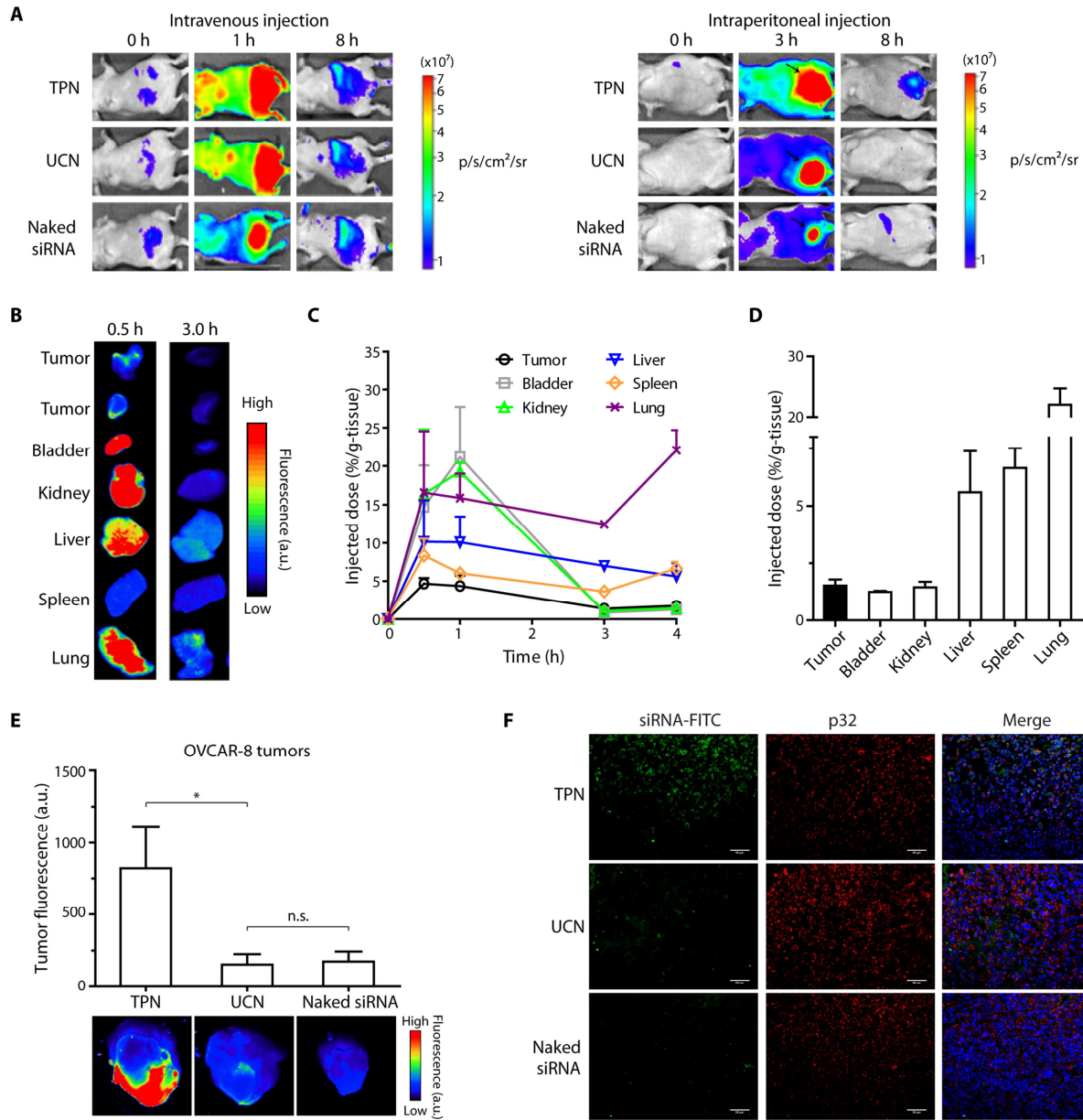


Figure S6. Biodistribution of TPN. (A) Whole-animal fluorescence imaging at multiple time points after intravenous or intraperitoneal injection of TPN or UCN carrying fluorescently labeled siRNA or naked siRNAs ($n = 3$ per group). The same representative animal from each group is shown for each time point. (B) Mice bearing subcutaneous MDA-MB-435 tumor xenografts were injected intravenously with TPN. At 0.5 and 3 h after injection, organs and tumors were harvested from mice and imaged for siRNA fluorescence. Representative tissues are shown in pseudocolor. (C) Quantification of injected TPN dose accumulated in tissue at various time points after intravenous bolus injection of TPN. Numerical values were computed based on a standard curve using uninjected organs spiked with known amounts of fluorescent siRNA. Data are averages \pm s.d. ($n = 4-6$ per organ per time point). (D) Proportion of injected dose accumulated per gram of tissue for explanted organs and tumors. Data are averages \pm s.d. ($n = 4-$

6 per organ). **(E)** TPN uptake in mice bearing OVCAR-8 tumor xenografts. Quantification of siRNA fluorescence per tumor cross-sectional area and corresponding whole-tumor fluorescence images are shown. Tumors were harvested 4 h after injection of TPN, UCN, or naked siRNA. Data are averages \pm s.d. ($n = 4$). $*P < 0.05$, n.s. not significant, by one-way ANOVA. **(F)** Immunofluorescence staining of TPN, UCN, or naked FITC-labeled siRNA delivered intravenously to OVCAR-8 ovarian tumor xenografts. Scale bars, 50 μm .

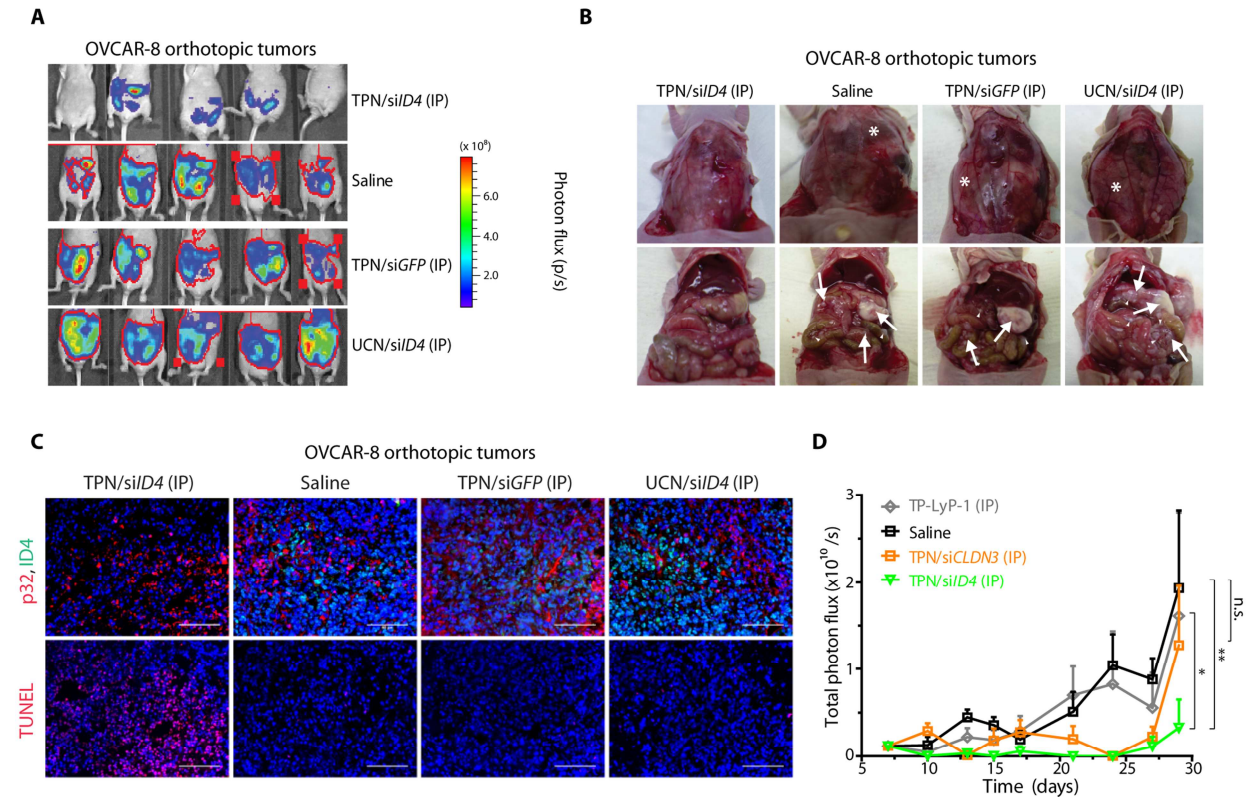


Figure S7. Therapeutic effects of *ID4* suppression in ovarian tumor-bearing mice. (A) Bioluminescence imaging of OVCAR-8 cells expressing firefly luciferase in mice bearing orthotopic OVCAR-8 ovarian tumor xenografts at day 40 ($n = 5$ per treatment group). (B) Photographs of representative OVCAR-8 tumor bearing mice from each cohort upon necropsy at day 60. Asterisks indicate the presence of hemorrhagic ascites in the peritoneal cavity. Arrows indicate the presence of disseminated ovarian tumor nodules. (C) Tumor sections harvested from all 4 cohorts on day 40 were co-stained for p32 and ID4 and stained for apoptotic cell death by TUNEL. (D) Comparison of the therapeutic efficacy of *Claudin-3* (*CLDN3*) versus *ID4* suppression by TPN in mice bearing orthotopic OVCAR-8 human ovarian tumor xenografts. Mice were treated every 3 days with TPN/si*CLDN3* or TPN/si*ID4*. Control cohorts received either saline or TP-LyP-1 peptide without siRNA. Data are averages \pm s.d. ($n = 5$ animals per group). * $p < 0.05$, ** $p < 0.01$, n.s., not significant, one-way ANOVA.

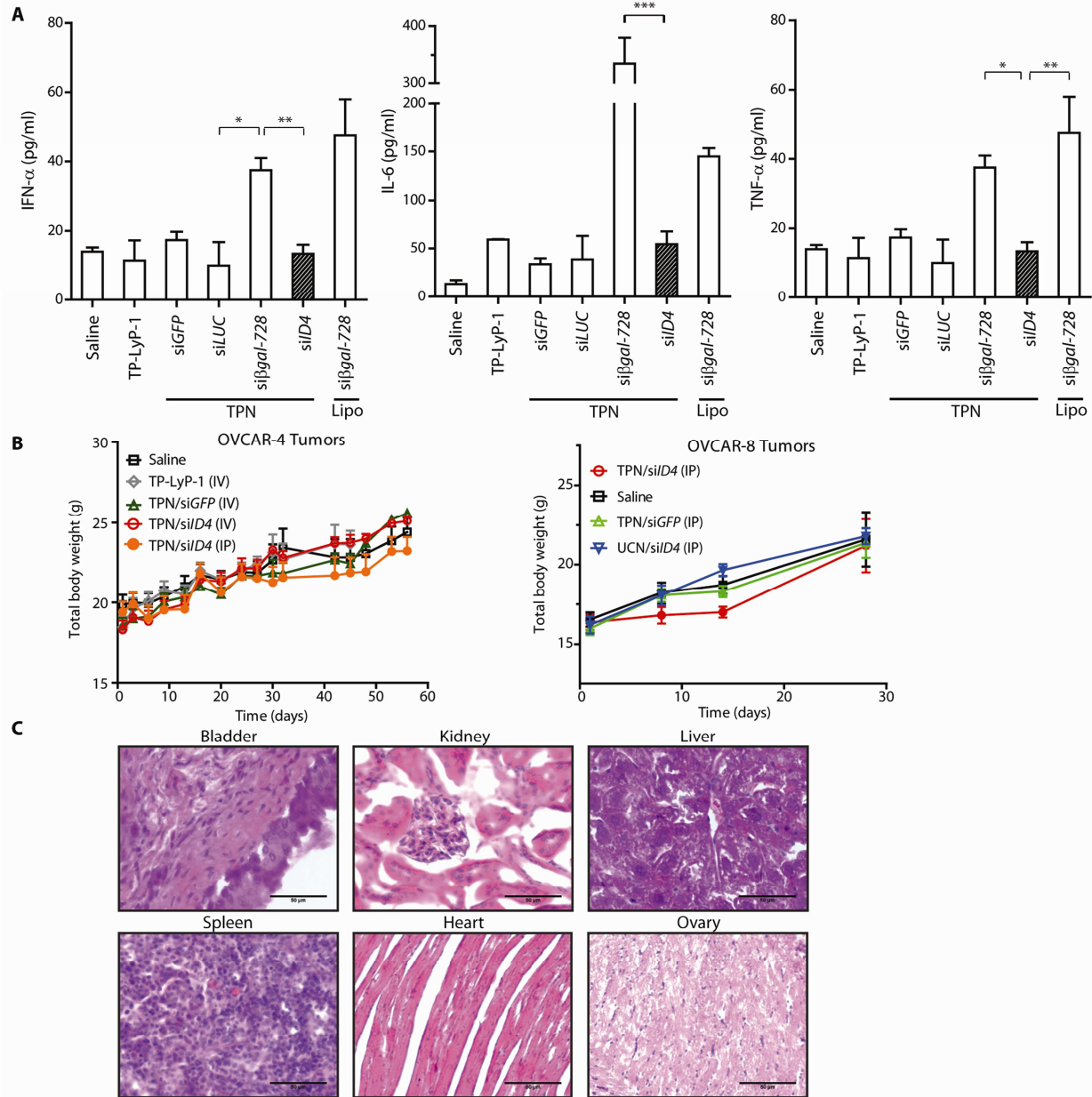


Figure S8. Lack of toxicity of siD4. (A) Balb/c mice bearing ovarian tumors were injected intraperitoneally with TPNs. After 6 hours, serum samples were tested for levels of IFN- α , IL-6, and TNF- α by ELISA. *siβgal-728* was used as a positive control for nonspecific immunostimulation. Data are averages \pm s.d. ($n = 5-8$ mice per group). * $p < 0.05$, ** $p < 0.01$, *** $p < 0.001$, by one-way ANOVA. (B) Total body weight of OVCAR-4 subcutaneous tumor xenograft-bearing mice and OVCAR-8 orthotopic tumor xenograft-bearing mice over the course of therapy. Data are averages \pm s.d. ($n = 5$ mice per group). (C) Absence of general tissue toxicity after TPN treatment. Organs were harvested from OVCAR-8 tumor-bearing mice after treatment for 40 days (5 mg siRNA/kg/injection) and stained with H&E. Scale bars, 50 μ m.

SUPPLEMENTARY TABLES

Table S1: List of amplified genes with at least one shRNA that score with a $P < 0.05$.

Gene	Z-score of best-scoring shRNA	P-value of best-scoring shRNA	Number of shRNAs with $P < 0.05$
<i>AKRIC2</i>	-4.25	0.0000107	1
<i>OPA1</i>	-4.227	0.0000118	1
<i>RPS27A</i>	-3.83	0.0000642	2
<i>SH3BP5L</i>	-3.729	0.0000962	1
<i>EGFLAM</i>	-3.68	0.000117	2
<i>EIF3G</i>	-3.63	0.000142	3
<i>RBM17</i>	-3.573	0.000177	2
<i>FBXO18</i>	-3.421	0.000312	1
<i>BOP1</i>	-3.386	0.000355	1
<i>RAD52</i>	-3.329	0.000435	1
<i>TBCE</i>	-3.292	0.000497	1
<i>MUT</i>	-3.274	0.00053	1
<i>ERBB3</i>	-3.258	0.000561	2
<i>PPIE</i>	-3.229	0.000622	1
<i>ZNF777</i>	-3.175	0.00075	1
<i>DLG5</i>	-3.172	0.000756	1
<i>PITRM1</i>	-3.153	0.000808	1
<i>IQGAP1</i>	-3.028	0.00123	2
<i>TRIP13</i>	-3.026	0.00124	3
<i>SMARCC2</i>	-3.004	0.00133	2
<i>EIF4A3</i>	-2.995	0.00137	2
<i>BIRC5</i>	-2.983	0.00143	2
<i>GIMAP5</i>	-2.981	0.00144	2
<i>FBXO4</i>	-2.971	0.00148	1
<i>KRAS</i>	-2.964	0.00152	5
<i>TPX2</i>	-2.938	0.00165	1
<i>UGP2</i>	-2.897	0.00188	1
<i>RPL37</i>	-2.894	0.0019	3
<i>HSP90AB1</i>	-2.888	0.00194	1
<i>ARFRP1</i>	-2.869	0.00206	1
<i>PCYT2</i>	-2.856	0.00215	2
<i>CC2D1A</i>	-2.848	0.0022	1
<i>XRCC2</i>	-2.838	0.00227	1
<i>GUCA1A</i>	-2.814	0.00245	1
<i>SKP2</i>	-2.768	0.00282	1
<i>ACYP2</i>	-2.767	0.00283	2
<i>TXNDC5</i>	-2.732	0.00315	1

<i>PDCD6</i>	-2.721	0.00325	1
<i>SC5DL</i>	-2.707	0.0034	2
<i>HIBCH</i>	-2.671	0.00378	1
<i>BTBD6</i>	-2.642	0.00412	1
<i>KCNK16</i>	-2.624	0.00435	2
<i>ST8SIA2</i>	-2.595	0.00473	1
<i>EXOSC4</i>	-2.59	0.00479	1
<i>CAPSL</i>	-2.579	0.00495	1
<i>NFIX</i>	-2.555	0.00531	1
<i>FOXK2</i>	-2.528	0.00574	1
<i>RAD1</i>	-2.524	0.00581	1
<i>AHRR</i>	-2.524	0.0058	1
<i>RBM24</i>	-2.514	0.00596	1
<i>GPS1</i>	-2.509	0.00605	2
<i>RIOK1</i>	-2.509	0.00605	1
<i>CDH9</i>	-2.49	0.0064	1
<i>VRK2</i>	-2.488	0.00642	2
<i>CACNA1A</i>	-2.462	0.0069	1
<i>BCL2L1</i>	-2.455	0.00705	2
<i>NAB1</i>	-2.44	0.00735	1
<i>IL7R</i>	-2.427	0.00761	1
<i>ZFR</i>	-2.419	0.00777	1
<i>WDR92</i>	-2.416	0.00784	1
<i>ACTG1</i>	-2.411	0.00795	2
<i>APOD</i>	-2.369	0.00893	1
<i>ZNF642</i>	-2.36	0.00915	1
<i>PEX13</i>	-2.359	0.00915	1
<i>FANCL</i>	-2.345	0.00952	1
<i>AKT1</i>	-2.337	0.00972	1
<i>KCNK17</i>	-2.329	0.00993	1
<i>MDH1</i>	-2.324	0.0101	1
<i>FBXO11</i>	-2.309	0.0105	1
<i>MYL6</i>	-2.308	0.0105	1
<i>MYST3</i>	-2.294	0.0109	1
<i>SCRT1</i>	-2.293	0.0109	1
<i>VEGFA</i>	-2.292	0.0109	1
<i>CAPN11</i>	-2.289	0.0111	1
<i>ICAM1</i>	-2.288	0.0111	1
<i>LIFR</i>	-2.267	0.0117	1
<i>FGD4</i>	-2.254	0.0121	1
<i>ADAMTS12</i>	-2.233	0.0128	1
<i>SSRI</i>	-2.22	0.0132	1
<i>CALM2</i>	-2.212	0.0135	1

<i>CACNA2D4</i>	-2.204	0.0138	1
<i>ADSSL1</i>	-2.203	0.0138	1
<i>LMBR1</i>	-2.198	0.014	1
<i>NR2F2</i>	-2.197	0.014	1
<i>MTA3</i>	-2.194	0.0141	1
<i>AFMID</i>	-2.168	0.0151	1
<i>RPS16</i>	-2.163	0.0153	1
<i>ID11</i>	-2.159	0.0154	1
<i>CSNK1D</i>	-2.158	0.0155	1
<i>TTC23</i>	-2.158	0.0155	1
<i>THRAP3</i>	-2.157	0.0155	1
<i>WNK1</i>	-2.156	0.0155	1
<i>CCND3</i>	-2.155	0.0156	1
<i>DEK</i>	-2.145	0.016	1
<i>POLB</i>	-2.141	0.0162	1
<i>MYL6B</i>	-2.136	0.0163	1
<i>PRB4</i>	-2.136	0.0164	1
<i>GTPBP4</i>	-2.123	0.0169	2
<i>EFEMP1</i>	-2.12	0.017	1
<i>EFCAB2</i>	-2.119	0.017	1
<i>MDFI</i>	-2.114	0.0173	1
<i>TSTA3</i>	-2.114	0.0172	1
<i>SUPT5H</i>	-2.106	0.0176	1
<i>HAAO</i>	-2.102	0.0178	2
<i>SENP5</i>	-2.097	0.018	1
<i>ID4</i>	-2.095	0.0181	1
<i>NNT</i>	-2.087	0.0184	1
<i>GNMT</i>	-2.084	0.0186	1
<i>SRMS</i>	-2.069	0.0193	1
<i>SLCO3A1</i>	-2.058	0.0198	1
<i>KCNK5</i>	-2.058	0.0198	1
<i>RAC3</i>	-2.052	0.0201	1
<i>HSF1</i>	-2.047	0.0204	1
<i>NCBP2</i>	-2.046	0.0204	1
<i>TAS2R43</i>	-2.045	0.0204	1
<i>E2F3</i>	-2.043	0.0205	1
<i>SRBD1</i>	-2.028	0.0213	1
<i>LMLN</i>	-2.013	0.0221	2
<i>ZFP36</i>	-2.002	0.0226	1
<i>HOXD4</i>	-2.001	0.0227	1
<i>PA2G4</i>	-1.998	0.0229	1
<i>PGS1</i>	-1.996	0.023	1
<i>ALDH1A3</i>	-1.983	0.0237	2

<i>RHEB</i>	-1.983	0.0237	1
<i>PRKAA1</i>	-1.982	0.0237	3
<i>CCL28</i>	-1.978	0.0239	1
<i>SOCS5</i>	-1.971	0.0244	3
<i>GUCA1B</i>	-1.955	0.0253	1
<i>CABYR</i>	-1.951	0.0255	1
<i>HOXD13</i>	-1.949	0.0257	1
<i>HOXD10</i>	-1.948	0.0257	1
<i>TFEB</i>	-1.948	0.0257	1
<i>PCMTD2</i>	-1.945	0.0259	1
<i>TACC3</i>	-1.936	0.0264	1
<i>TYK2</i>	-1.935	0.0265	1
<i>MSH2</i>	-1.927	0.027	1
<i>MYCL1</i>	-1.916	0.0277	1
<i>GIMAP4</i>	-1.916	0.0277	1
<i>CAP1</i>	-1.902	0.0286	1
<i>C6orf105</i>	-1.902	0.0286	1
<i>RNASE8</i>	-1.901	0.0286	1
<i>CDH10</i>	-1.898	0.0288	1
<i>PNO1</i>	-1.889	0.0294	2
<i>RTEL1</i>	-1.888	0.0295	2
<i>RANBP9</i>	-1.888	0.0295	1
<i>RARRES2</i>	-1.884	0.0298	1
<i>NET1</i>	-1.882	0.0299	1
<i>DCXR</i>	-1.881	0.03	1
<i>COL14A1</i>	-1.881	0.03	1
<i>KCNQ2</i>	-1.88	0.03	1
<i>PLA2G7</i>	-1.878	0.0302	2
<i>RICTOR</i>	-1.875	0.0304	1
<i>IL27RA</i>	-1.874	0.0305	1
<i>TFRC</i>	-1.863	0.0312	1
<i>ICAM4</i>	-1.862	0.0313	1
<i>TBC1D16</i>	-1.86	0.0315	1
<i>FSHR</i>	-1.856	0.0317	1
<i>SLC1A3</i>	-1.847	0.0324	2
<i>GULP1</i>	-1.842	0.0327	1
<i>CPSF1</i>	-1.842	0.0327	1
<i>ZMYND11</i>	-1.839	0.033	1
<i>AMACR</i>	-1.832	0.0334	1
<i>TMOD4</i>	-1.824	0.0341	1
<i>CHD2</i>	-1.809	0.0352	1
<i>POLR3A</i>	-1.808	0.0353	1
<i>NPC1</i>	-1.804	0.0356	1

<i>ENPP5</i>	-1.801	0.0358	1
<i>GCNT2</i>	-1.8	0.036	1
<i>MYO9B</i>	-1.8	0.0359	1
<i>TAF4B</i>	-1.797	0.0361	1
<i>ARNT</i>	-1.796	0.0362	1
<i>OR2T10</i>	-1.792	0.0366	1
<i>ABCB8</i>	-1.786	0.037	1
<i>TRIM58</i>	-1.785	0.0371	1
<i>TAS2R42</i>	-1.775	0.0379	1
<i>NFYA</i>	-1.772	0.0382	1
<i>REL</i>	-1.766	0.0387	2
<i>MYC</i>	-1.754	0.0397	1
<i>PTK7</i>	-1.745	0.0405	1
<i>ZNF670</i>	-1.744	0.0405	1
<i>ILF3</i>	-1.744	0.0406	1
<i>AKR1C1</i>	-1.743	0.0407	1
<i>CHRNA4</i>	-1.741	0.0408	1
<i>SIX3</i>	-1.739	0.041	1
<i>GTF2A1L</i>	-1.737	0.0412	1
<i>SLC35B3</i>	-1.732	0.0416	1
<i>BAIAP2</i>	-1.732	0.0416	1
<i>IKZF4</i>	-1.725	0.0423	1
<i>GALNTL5</i>	-1.717	0.043	1
<i>STAT1</i>	-1.717	0.043	1
<i>ETAA1</i>	-1.711	0.0435	1
<i>RAB25</i>	-1.709	0.0437	1
<i>CDC5L</i>	-1.707	0.044	1
<i>UBR2</i>	-1.702	0.0444	1
<i>NLRP3</i>	-1.695	0.045	1
<i>GIMAP8</i>	-1.695	0.045	1
<i>RAB40B</i>	-1.689	0.0456	1
<i>SLC45A2</i>	-1.688	0.0457	1
<i>KIAA0226</i>	-1.684	0.0461	1
<i>MYCBP</i>	-1.684	0.0461	1
<i>FKBP7</i>	-1.676	0.0469	1
<i>RCCD1</i>	-1.67	0.0475	1
<i>TUBB8</i>	-1.666	0.0479	1
<i>RAVER1</i>	-1.662	0.0482	1
<i>TIMM50</i>	-1.652	0.0493	1
<i>P4HB</i>	-1.645	0.05	1

Table S2. Sequence and characterization of tandem peptides. The myr- prefix denotes N-terminal myristoylation. Lysine (K) residues were labeled with a fluorophore (TAMRA). Mean diameter was based on DLS measurements in PBS. For zeta-potential and diameter, $n = 4$ independent measurements. Peptide abbreviations are as follows: (dR) $_n$, oligoarginine, where n is the number of d-Arginine residues; PEN, penetratin; TAT, HIV TAT (48-60); TP, transportan; VP22, HSV-1 VP22 protein.

Name	Sequence	Average ζ -potential \pm SD (mV)	Average diameter \pm SD (nm)
m3R	myr-(dR) ₃ GGGGK(TAMRA)CGNKRTRGC	21.8 \pm 5.0	209.0 \pm 40.5
m6R	myr-(dR) ₆ GGGGK(TAMRA)CGNKRTRGC	27.3 \pm 4.0	151.0 \pm 11.1
m9R	myr-(dR) ₉ GGGGK(TAMRA)CGNKRTRGC	36.6 \pm 7.1	207.8 \pm 19.6
m12R	myr-(dR) ₁₂ GGGGK(TAMRA)CGNKRTRGC	27.6 \pm 15.0	191.2 \pm 17.9
m15R	myr-(dR) ₁₅ GGGGK(TAMRA)CGNKRTRGC	36.0 \pm 7.5	377.2 \pm 49.4
mPEN	myr- RQIKIWFQNRRMKWKKGGGGK(TAMRA)CGNKRTRGC	29.0 \pm 5.1	337.6 \pm 54.9
mTAT	myr-GRKKRRQRRRQYKGGGGK(TAMRA)CGNKRTRGC	35.8 \pm 8.0	194.6 \pm 43.6
mTP	myr- GWTLNSAGYLLGKINLKALAALAKKILGGGGK(TAMRA) CGNKRTRGC	31.9 \pm 3.7	343.6 \pm 32.3
mVP22	myr- DAATATRGRSAASRPTERPRAPARSASRPRRPVDGGGGK (TAMRA)CGNKRTRGC	30.8 \pm 4.8	233.0 \pm 58.8